MLD-based MFSK Demodulation on MIMO Frequency Selective Fading Channel

Yasunori Iwanami
Dept. of Computer Science and Engineering
Nagoya Institute of Technology
Nagoya, Japan
E-mail: iwanami@nitech.ac.jp

Kenji Nakayama
Dept. of Computer Science and Engineering
Nagoya Institute of Technology
Nagoya, Japan
E-mail: nakayama@rose.nitech.ac.jp

Abstract— **In this paper, we have proposed the novel demodulation scheme of MFSK (M-ary Frequency Shift Keying) signals on MIMO frequency selective channel. For demodulating MIMO MFSK signals, we previously used the FDE (Frequency Domain Equalization) using CP (Cyclic Prefix). In order to further improve the BER characteristics, the novel scheme using MLD (Maximum Likelihood Detection) with ISI canceller and ZP (Zero Padding) has been considered. We further reduced the receiver complexity by replacing MLD with M algorithm. Through computer simulation, we have verified that the proposed scheme using M algorithm with ISI canceller exhibits the excellent BER characteristics compared with the FDE with CP.**

Keywords-MIMO, MFSK, ISI, IAI, MLD, M-algorithm, FDE, Multipath channel

I. INTRODUCTION

MFSK signal has the constant envelope property and is appropriate to be amplified by nonlinear amplifier with high power efficiency. However, as the MFSK is the nonlinear modulation scheme, the equalization at the receiver side has been difficult when it is subjected to frequency selective channels. On the other side, due to the increasing demand of high data rate and reliable data transmission, MIMO (Multiple Input Multiple Output) schemes with multiple transmit and receive antennas become quite popular recently. The conventional MIMO scheme processes the received signals using the linear matrix processing. However it has been difficult to apply the linear processing to the nonlinear modulation such as MIMO MFSK, and accordingly there was almost no research on MIMO FSK. So, we aimed to develop the MIMO FSK transmission scheme.

TABLE I LIST of PARAMETERS

N_S : Transmission block length
N_G : Number of zero symbols
$2c$: Number of samples per symbol
T_s : Symbol duration
Δt : Sampling interval; $\Delta t = T_s/(2c)$
k : time index; present time
$(L-1)T_s$: Maximum symbol delay time
M : Number of modulation level
n_T : Number of transmit antenna
n_R : Number of receive antenna
J : Total number of delay paths
$\Delta\tau$: Delay path interval
M_c : Parameter of M algorithm

We had already shown that the FDE (Frequency Domain Equalization) scheme using CP (Cyclic Prefix) [1] is applicable to the signal separation and equalization of MIMO MFSK signals [2]-[4], where the FDE is done before the demodulation process of MFSK signal. This method was originally developed for SISO (Single Input Single Output) FSK signals [5]. In this paper, in order to improve the BER characteristics as well as the receiver complexity of previously developed schemes [2]-[4], we consider here the demodulation of MIMO MFSK where the MLD with ISI canceller using ZP is adopted. The receiver minimizes the Euclidian distance between the receive signal and the receive signal replica of candidate transmit signal. Moreover, we have replaced the MLD by M-algorithm to further reduce the receiver complexity. We have verified that the proposed receiver structure using M-algorithm with ISI canceller exhibits the excellent BER characteristics compared with the FDE with CP.

II. MIMO MFSK DETECTION USING MLD WITH ISI CANCELLER

We consider the detection scheme of MFSK using MLD with ISI canceller in time domain, which improves the BER performance compared with the FDE scheme using CP [2]-[4]. In Fig. 1, we show the block diagram of MIMO MFSK transmission scheme having the receiver using MLD with ISI canceller operating in time domain. At the transmitter side, as shown in Fig. 2, N_S MFSK modulated symbols with N_G ZP symbols (zero symbols) are transmitted from each transmit antenna. The ZP symbols are required to circumvent the Inter Block Interference (IBI) between the successive blocks caused by the multipath delay. The ZP is also used to reset the initial phase of continuous phase MFSK signal to be zero at the beginning of the transmit block. The reset of initial phase of continuous phase MFSK signal is necessary for generating the receive signal replica for MLD with phase synchronization at the receiver. Terminating the transmit symbol block by ZP is also useful to prevent the error propagation caused by erroneous ISI cancellation at the receiver. At the receiver side, the detection of Inphase and Quadrature (I and Q) components of MFSK symbols with the block length of $(N_S + N_G)T_s$ is done to get the complex baseband symbols. Then the discrete time samples at the sampling rate of $2c$ per one symbol duration T_s are taken in time domain, i.e., the sampling interval of

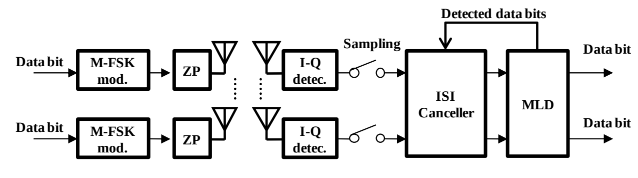

Fig. 1 Block diagram of transmit and receive system of MIMO MFSK using MLD with ISI canceller on frequency selective channel

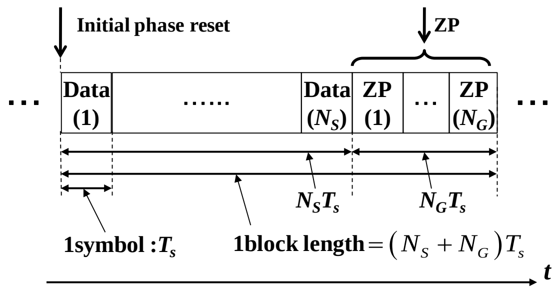

Fig. 2 Transmit signal block and Zero Padding (ZP) at the transmitter side

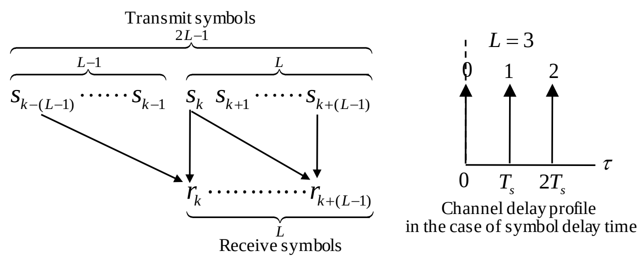

Fig. 3 Relation between transmit and receive signals on multipath delay channel in the case of SISO and symbol delay time

$\Delta t = T_s/(2c)$. We define the present time index as k and the maximum symbol delay time due to multipath channel as $(L-1)T_s$. For simplicity, we also assume the SISO (1×1) transmission in the subsequent illustration. As shown in Fig. 3, to detect the symbol transmitted at time k using MLD, we need the total L receive symbols over the symbol time $k \sim k+(L-1)$, because the transmit signal at time k spreads over the receive symbols during $k \sim k+(L-1)$. As those L receive symbols contain the transmit symbol components over $k-(L-1)$ to $k+(L-1)$, it is required for the MLD to search all the transmit symbol pattern over $(2L-1)$ symbols. Accordingly, the number of searches in MLD becomes $M^{(2L-1)}$ in the case of SISO [6].

We now consider the symbol time k in Fig. 3 as the first data symbol in Fig. 2, i.e., we let $k=1$. Then all the transmit symbols $s_{k-(L-1)},\cdots,s_{k-1}$ are zero, because they are included in ZP duration. After receiving total L symbols of $r_k,\cdots\cdots,r_{k+(L-1)}$, the first transmit symbol s_k is detected using the MLD. The next r_{k+L} is then received and the second transmit symbol s_{k+1} is also detected by using MLD. However, the ISI components caused by the first transmit symbol s_k is removed through the ISI canceller before the MLD by subtracting the hard receive replicas from the received signals. Similarly, after receiving the next receive symbol r_{k+L+1}, the third transmit symbol s_{k+2} is detected by using MLD, however the ISI components due to s_k and s_{k+1} are cancelled by the ISI canceller before the MLD operation. Likewise, the subsequent transmit symbol $s_{k+i}, i \geq 3 \sim N_S$ is detected using MLD, however the ISI components caused by the transmit symbols already detected are cancelled by the ISI canceller. The ISI cancellation reduces the number of searches of MLD from $M^{(2L-1)}$ to M^L. The metric of MLD is taken as the squared Euclidian distance between the receive symbols after ISI cancellation and the receive symbol replicas corresponding to the candidate transmit symbols over L symbol duration. The transmit symbol is then detected so as to minimizes the metric of MLD [6].

The proposed signal separation and equalization algorithm is illustrated in detail as follows. The channel matrix $\boldsymbol{H}$ is expressed as

$$\boldsymbol{H}=\begin{bmatrix} \boldsymbol{h}_0 & \cdots & \boldsymbol{h}_l & \cdots & \boldsymbol{h}_{J-1} & 0 & \cdots & 0 \\ 0 & & & & & & 0 & \vdots \\ \vdots & 0 & \boldsymbol{h}_0 & \cdots & \boldsymbol{h}_l & \cdots & \boldsymbol{h}_{J-1} & 0 \\ 0 & \cdots & 0 & \boldsymbol{h}_0 & \cdots & \boldsymbol{h}_l & \cdots & \boldsymbol{h}_{J-1} \end{bmatrix} \tag{1}$$

where n_T and n_R are the numbers of transmit and receive antennas respectively. The element $\boldsymbol{h}_l$ in (1) is also the matrix expressed as

$$\boldsymbol{h}_l=\begin{bmatrix} h_{11}^{(l)} & h_{12}^{(l)} & \cdots & h_{1n_T}^{(l)} \\ h_{21}^{(l)} & h_{22}^{(l)} & \cdots & h_{2n_T}^{(l)} \\ \vdots & \vdots & & \vdots \\ h_{n_R 1}^{(l)} & h_{n_R 2}^{(l)} & \cdots & h_{n_R n_T}^{(l)} \end{bmatrix},\quad l=0,\cdots,J-1 \tag{2}$$

where $h_{ji}^{(l)}$ is the complex channel gain of l-th delayed path from transmit antenna i to receive antenna j and J is the total number of delay paths.

The delay profile between transmit antenna i and receive antenna j is shown in Fig. 4, where the maximum delay time is $(J-1)\Delta\tau$.

The transmit symbol vector, the receive symbol vector and the receive noise vector at symbol time k are expressed as follows.

$$\left.\begin{aligned} &\text{Transmit symbol vector at symbol time } k:\\ &\boldsymbol{X}_k=\left(\boldsymbol{x}_{k,2c},\cdots,\boldsymbol{x}_{k,q},\cdots,\boldsymbol{x}_{k,1}\right)^T,\ \boldsymbol{x}_{k,q}=\left(x_{k,q}^{(1)},\cdots,x_{k,q}^{(i)},\cdots,x_{k,q}^{(n_T)}\right)^T\\ &\text{Receive symbol vector at symbol time } k:\\ &\boldsymbol{Y}_k=\left(\boldsymbol{y}_{k,2c},\cdots,\boldsymbol{y}_{k,q},\cdots,\boldsymbol{y}_{k,1}\right)^T,\ \boldsymbol{y}_{k,q}=\left(y_{k,q}^{(1)},\cdots,y_{k,q}^{(j)},\cdots,y_{k,q}^{(n_R)}\right)^T\\ &\text{Receive noise vector at symbol time } k:\\ &\boldsymbol{N}_k=\left(\boldsymbol{n}_{k,2c},\cdots,\boldsymbol{n}_{k,q},\cdots,\boldsymbol{n}_{k,1}\right)^T,\ \boldsymbol{n}_{k,q}=\left(n_{k,q}^{(1)},\cdots,n_{k,q}^{(j)},\cdots,n_{k,q}^{(n_R)}\right)^T \end{aligned}\right\}(3)$$

where the element vector $\boldsymbol{x}_{k,q}$ in $\boldsymbol{X}_k$ is the sampled

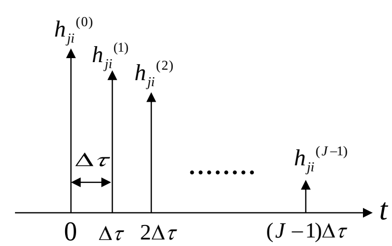

Fig. 4 Delay profile between transmit antenna i and receive antenna j on MIMO frequency selective channel

transmit vector at time $(q-1)\Delta t$ in symbol time k with $q = 1 \sim 2c$ and $\Delta t = T_s/(2c)$. Accordingly, one symbol duration T_s is sampled at every small time interval Δt. For example, $16\ (=2c)$ sample vectors $\boldsymbol{x}_{k,16}, \cdots, \boldsymbol{x}_{k,q}, \cdots, \boldsymbol{x}_{k,1}$ are obtained for $\boldsymbol{X}_k$. Also $x_{k,q}^{(i)}$ in $\boldsymbol{x}_{k,q}$ is the sampled transmit symbol from transmit antenna i at time $(q-1)\Delta t$ in symbol time k. $\boldsymbol{y}_{k,q}$ in $\boldsymbol{Y}_k$, $y_{k,q}^{(i)}$ in $\boldsymbol{y}_{k,q}$, $\boldsymbol{n}_{k,q}$ in $\boldsymbol{N}_k$ and $n_{k,q}^{(i)}$ in $\boldsymbol{n}_{k,q}$ have the same meaning as $\boldsymbol{x}_{k,q}$ in $\boldsymbol{X}_k$ and $x_{k,q}^{(i)}$ in $\boldsymbol{x}_{k,q}$.

The transmit and receive equation is expressed as

$$\begin{aligned}\left(\boldsymbol{Y}_{k+(L-1)}, \cdots, \boldsymbol{Y}_k\right)^T &= \boldsymbol{H}\left(\boldsymbol{X}_{k+(L-1)}, \cdots, \boldsymbol{X}_k, \cdots, \boldsymbol{X}_{k-(L-1)}\right)^T \\ &\quad + \left(\boldsymbol{N}_{k+(L-1)}, \cdots, \boldsymbol{N}_k\right)^T\end{aligned} \tag{4}$$

where L is $L = \lceil (J-1)\Delta\tau / T_s \rceil + 1$ and $\lceil x \rceil$ denotes the minimum integer number greater than or equal to x. $(L-1)T_s$ also means the maximum symbol delay time.

We further illustrate the transmit and receive equation in detail by setting $n_T = n_R = 2$, $L = 2$ and $J = 2c$ for simplicity of explanation.

The element $y_{p,q}^{(1)}, y_{p,q}^{(2)},\ p = k, \cdots, k+(L-1),\ q = 1, \cdots, 2c$ of receive vector $\boldsymbol{y}_p^{(j)}$ in (3) are represented as follows.

$$\left.\begin{aligned}
y_{p,1}^{(1)} &= \left\{h_{11}^{(0)} x_{p,1}^{(1)} + h_{11}^{(1)} x_{p-1,2c}^{(1)} + \cdots + h_{11}^{(2c-1)} x_{p-1,2}^{(1)}\right\} \\
&\quad + \left\{h_{12}^{(0)} x_{p,1}^{(2)} + h_{12}^{(1)} x_{p-1,2c}^{(2)} + \cdots + h_{12}^{(2c-1)} x_{p-1,2}^{(2)}\right\} + n_{p,1}^{(1)} \\
&\vdots \\
y_{p,2c}^{(1)} &= \left\{h_{11}^{(0)} x_{p,2c}^{(1)} + h_{11}^{(1)} x_{p,2c-1}^{(1)} + \cdots + h_{11}^{(2c-1)} x_{p,1}^{(1)}\right\} \\
&\quad + \left\{h_{12}^{(0)} x_{p,2c}^{(2)} + h_{12}^{(1)} x_{p,2c-1}^{(2)} + \cdots + h_{12}^{(2c-1)} x_{p,1}^{(2)}\right\} + n_{p,2c}^{(1)} \\
y_{p,1}^{(2)} &= \left\{h_{21}^{(0)} x_{p,1}^{(1)} + h_{21}^{(1)} x_{p-1,2c}^{(1)} + \cdots + h_{21}^{(2c-1)} x_{p-1,2}^{(1)}\right\} \\
&\quad + \left\{h_{22}^{(0)} x_{p,1}^{(2)} + h_{22}^{(1)} x_{p-1,2c}^{(2)} + \cdots + h_{22}^{(2c-1)} x_{p-1,2}^{(2)}\right\} + n_{p,1}^{(2)} \\
&\vdots \\
y_{p,2c}^{(2)} &= \left\{h_{12}^{(0)} x_{p,2c}^{(1)} + h_{12}^{(1)} x_{p,2c-1}^{(1)} + \cdots + h_{12}^{(2c-1)} x_{p,1}^{(1)}\right\} \\
&\quad + \left\{h_{22}^{(0)} x_{p,2c}^{(2)} + h_{22}^{(1)} x_{p,2c-1}^{(2)} + \cdots + h_{22}^{(2c-1)} x_{p,1}^{(2)}\right\} + n_{p,2c}^{(2)}
\end{aligned}\right\} \tag{5}$$

Here we elaborate on the elements $x_{k,1}^{(1)}, \cdots, x_{k,2c}^{(1)}$ of the transmit symbol vector $\boldsymbol{x}_k^{(1)}$ from transmit antenna 1 and $x_{k,1}^{(2)}, \cdots, x_{k,2c}^{(2)}$ of the transmit symbol vector $\boldsymbol{x}_k^{(2)}$ from transmit antenna 2. The channel responses of transmit symbol vectors $\boldsymbol{x}_k^{(1)}$ and $\boldsymbol{x}_k^{(2)}$ spread over the receive symbol vectors $\boldsymbol{y}_k^{(1)}, \cdots, \boldsymbol{y}_{k+(L-1)}^{(1)}$ and $\boldsymbol{y}_k^{(2)}, \cdots, \boldsymbol{y}_{k+(L-1)}^{(2)}$ with the maximum symbol delay time of $(L-1)T_s$ as illustrated in Fig. 3. In order to detect the transmit symbol vectors $\boldsymbol{x}_k^{(1)}$ and $\boldsymbol{x}_k^{(2)}$, the ISI components due to already detected symbols from symbol time $k-(L-1) \sim k-1$ can be removed from the receive vectors of $\boldsymbol{y}_k^{(1)}, \cdots, \boldsymbol{y}_{k+(L-1)}^{(1)}$ and $\boldsymbol{y}_k^{(2)}, \cdots, \boldsymbol{y}_{k+(L-1)}^{(2)}$. The ISI cancelling vector $\tilde{\boldsymbol{Y}}_p$ at symbol time p is expressed as

$$\tilde{\boldsymbol{Y}}_p = \left(\tilde{\boldsymbol{y}}_p^{(1)}, \cdots, \tilde{\boldsymbol{y}}_p^{(n_R)}\right)^T,\ p = k, \cdots, k+(L-1) \tag{6}$$

where $\tilde{\boldsymbol{y}}_p^{(j)} = \left(\tilde{y}_{p,2c}^{(j)}, \cdots, \tilde{y}_{p,1}^{(j)}\right)^T$ is the element symbol vector for cancelling the ISI at receive antenna j at symbol time p. Using the already detected symbols during $k-(L-1) \sim k-1$ symbol period, $\tilde{\boldsymbol{Y}}_p$ in (6) is derived as

$$\left(\tilde{\boldsymbol{Y}}_{k+(L-1)}, \cdots, \tilde{\boldsymbol{Y}}_k\right)^T = \boldsymbol{H}\left(\overbrace{\boldsymbol{0}, \cdots, \boldsymbol{0}}^{L \text{ symbols}}, \overbrace{\tilde{\boldsymbol{X}}_{k-1}, \cdots, \tilde{\boldsymbol{X}}_{k-(L-1)}}^{(L-1) \text{ detected symbols}}\right)^T \tag{7}$$

where $\tilde{\boldsymbol{X}}_p,\ p = k-1, \cdots, k-(L-1)$ are the already detected results. Next, using $\tilde{\boldsymbol{Y}}_{k+(L-1)}, \cdots, \tilde{\boldsymbol{Y}}_k$ in (7), the ISI is cancelled as follows.

$$\hat{\boldsymbol{Y}}_p = \boldsymbol{Y}_p - \tilde{\boldsymbol{Y}}_p,\ p = k, \cdots, k+(L-1) \tag{8}$$

where $\hat{\boldsymbol{Y}}_p$ is the receive symbol vector after the ISI cancellation. Using the transmit signal $\boldsymbol{X}_p$, receive noise $\boldsymbol{N}_p$ and residual ISI component $\boldsymbol{\varepsilon}_p$, $\hat{\boldsymbol{Y}}_p,\ p = k, \cdots, k+(L-1)$ in (8) is also represented as

$$\begin{aligned}\left(\hat{\boldsymbol{Y}}_{k+(L-1)}, \cdots, \hat{\boldsymbol{Y}}_k\right)^T &= \boldsymbol{H}\left(\overbrace{\boldsymbol{X}_{k+(L-1)} \cdots, \boldsymbol{X}_k}^{L \text{ symbols}}, \overbrace{\boldsymbol{0}, \cdots, \boldsymbol{0}}^{(L-1) \text{ symbols}}\right)^T \\ &\quad + \left(\boldsymbol{N}_{k+(L-1)}, \cdots, \boldsymbol{N}_k\right)^T + \left(\boldsymbol{\varepsilon}_{k+(L-1)}, \cdots, \boldsymbol{\varepsilon}_k\right)^T\end{aligned} \tag{9}$$

The residual ISI component $\boldsymbol{\varepsilon}_p$ is $\boldsymbol{0}$, if the past decision results are correct. Also when the ISI cancellation is perfect and there is no noise, i.e., $\boldsymbol{N}_p = \boldsymbol{0}$, it holds

$$\left(\hat{\boldsymbol{Y}}_{k+(L-1)}, \cdots, \hat{\boldsymbol{Y}}_k\right)^T = \boldsymbol{H}\left(\overbrace{\boldsymbol{X}_{k+(L-1)} \cdots, \boldsymbol{X}_k}^{L \text{ symbols}}, \overbrace{\boldsymbol{0}, \cdots, \boldsymbol{0}}^{(L-1) \text{ symbols}}\right)^T \tag{10}$$

where $\boldsymbol{X}_{k+(L-1)}, \cdots, \boldsymbol{X}_k$ are transmit signals to be determined.

The transmit signal vector $\boldsymbol{X}_k$ at the present symbol time k is determined so as to minimize the squared Euclidian distance metric as shown below.

$$\boldsymbol{X}_k = \underset{\boldsymbol{X}_{k+(L-1)}, \cdots, \boldsymbol{X}_k}{\arg\min}\left[\left\|\left(\hat{\boldsymbol{Y}}_{k+(L-1)}, \cdots, \hat{\boldsymbol{Y}}_k\right)^T - \boldsymbol{H}\left(\overbrace{\boldsymbol{X}_{k+(L-1)} \cdots, \boldsymbol{X}_k}^{L \text{ symbols}}, \overbrace{\boldsymbol{0}, \cdots, \boldsymbol{0}}^{(L-1) \text{ symbols}}\right)^T\right\|^2\right] \tag{11}$$

The above equation is the MLD criterion by which all the transmit vector patterns of $\boldsymbol{X}_{k+(L-1)} \cdots, \boldsymbol{X}_k$ are searched to determine the transmit vector $\boldsymbol{X}_k$ at symbol time k. In minimizing the metric in (11), all the L transmit vectors from symbol time $k \sim k+(L-1)$ are simultaneously searched, however only the transmit vector $\boldsymbol{X}_k$ at symbol time k is determined as the demodulated output.

The BER characteristics of the proposed MLD with ISI canceller and the previously proposed FDE with CP are simulated under the simulation condition in Table II. The delay profile between each transmit and receive antenna is shown in Fig. 5.

We show the BER results in Fig. 6. From Fig. 6, comparing with the FDE scheme with CP, the proposed MLD with ISI canceller achieves the gain of 13 dB at

TABLE II SIMULATION CONDITION IN FIG. 6

Modulation	M-ary FSK (M=4)	
Modulation index h	$h = 0.7$	
Channel model between Tx and Rx antenna	Quasi-static Rayleigh fading channel with equal power 16 paths	
Interval of delay $\Delta\tau$	$\Delta\tau = T_s / 8$	
Number of antennas	SISO:1×1, MIMO:2×2	
Channel estimation	Perfect at receiver	
Signal separation and equalization	MLD with ISI canceller	FDE-CP (MMSE) with energy detection [2]~[4], [7], [8]
Number of divisions in one symbol: $2c$ ($T_s = 2c\Delta t$)	$2c$ =16	
Transmit block length $N_S T_s$	$4T_s$ ($N_S = 4$)	
Length of ZP or CP	$2T_s$ (ZP)	$2T_s$ (CP for FDE)
FFT size: $2c \times N_S$	----	64

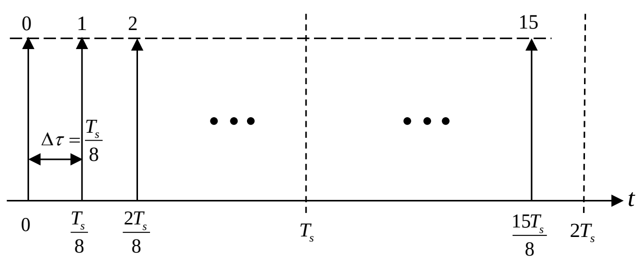

Fig. 5 Delay profile of multipath channel between each transmit and receive antenna in for Table II and Fig. 6

$\text{BER} = 10^{-5}$ for 1×1, and 16 dB for 2×2. Thus the proposed MLD with ISI canceller achieves far better equalization and signal separation capability than the previously proposed FDE scheme with CP. By removing the ISI caused by the symbols already detected, the MLD over L symbol span becomes available regardless of the block length. The long block length of $N_S T_s$ circumvents the degradation of transmission rate due to the insertion of ZP into the block.

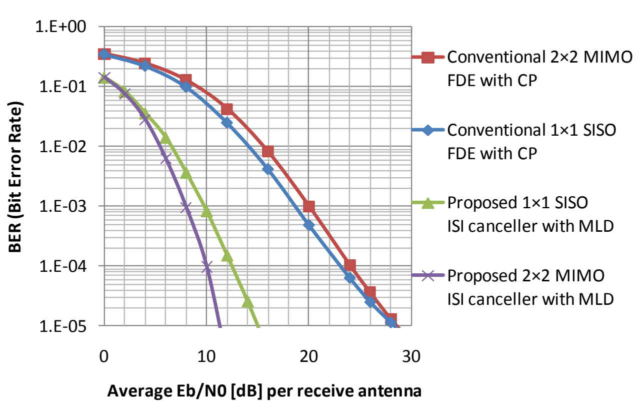

Fig. 6 BER characteristics of 4FSK (h=0.7) on MIMO quasi-static multipath channel

III. MIMO MFSK RECEIVER USING M ALGORITHM WITH ISI CANCELLER

In the receiver structure proposed in section II, the ISI canceller reduces the amount of calculation in MLD. However, the complexity of MLD is still high when the number of transmit antenna n_T and the maximum symbol delay time of $(L-1)T_s$ become large. This is because when $(L-1)T_s$ is large, the symbol vector $\boldsymbol{X}_k$ detected at the symbol time k influences L future symbols, thus the MLD window size L over the transmit symbol vectors $\boldsymbol{X}_k, \cdots, \boldsymbol{X}_{k+(L-1)}$ becomes large. In this section, we replace the MLD by the M algorithm to further reduce the amount of calculation in MLD. The M algorithm is the representative of breadth first search algorithms for the tree structure. Based on the MLD criterion in (11), the MLD metric is defined as

$$\left\| \left(\overbrace{\hat{\boldsymbol{Y}}_{k+(L-1)}, \cdots, \hat{\boldsymbol{Y}}_k}^{L \text{ symbols}} \right)^T - \boldsymbol{H} \left(\overbrace{\boldsymbol{X}_{k+(L-1)} \cdots, \boldsymbol{X}_k}^{L \text{ symbols}}, \overbrace{\boldsymbol{0}, \cdots, \boldsymbol{0}}^{(L-1) \text{ symbols}} \right)^T \right\|^2 \tag{12}$$

Now, we define the receive replica vector $\hat{\boldsymbol{Y}}'_p$, $p = k, \cdots, k+(L-1)$, as

$$\left(\overbrace{\hat{\boldsymbol{Y}}'_{k+(L-1)}, \cdots, \hat{\boldsymbol{Y}}'_p, \cdots, \hat{\boldsymbol{Y}}'_k}^{L \text{ symbols}} \right)^T = \boldsymbol{H} \left(\overbrace{\boldsymbol{X}_{k+(L-1)} \cdots, \boldsymbol{X}_k}^{L \text{ symbols}}, \overbrace{\boldsymbol{0}, \cdots, \boldsymbol{0}}^{(L-1) \text{ symbols}} \right)^T \tag{13}$$

where $\hat{\boldsymbol{Y}}'_p$ means the receive replica vector when assuming there is no ISI from the past symbol vectors transmitted. Using $\hat{\boldsymbol{Y}}'_p$ in (13), we can simplify eq.(12) as follows.

$$\sum_{p=k}^{k+(L-1)} \left\| \hat{\boldsymbol{Y}}_p - \hat{\boldsymbol{Y}}'_p \right\|^2 \tag{14}$$

Then we define the cumulative metric from the symbol time k to $i (=1, \cdots, L)$ as

$$\sum_{p=k}^{k+(i-1)} \left\| \hat{\boldsymbol{Y}}_p - \hat{\boldsymbol{Y}}'_p \right\|^2 \tag{15}$$

The cumulative metric in (15) at $i = L$ coincides with the MLD metric in (12). The above cumulative metric can be used as the likelihood criterion to determine the candidates of transmit symbol vectors up to i, i.e., $\boldsymbol{X}_{k+(i-1)}, \cdots, \boldsymbol{X}_k$. Using this cumulative metric, the transmit symbol vectors at each step i are selected from the total M_c (parameter of M algorithm) candidates. The parameter i is increased at each step. The total number of searches in M algorithm becomes $\{1+(L-1)M_c\} \times M^{n_T}$, where M is the number of modulation levels. On the other hand, the total number of searches in MLD in section II is $M^{n_T L}$. By using M algorithm, the total number of searches are reduced greatly, because the parameter of L is not included in the exponent.

To illustrate the M algorithm in the proposed scheme in detail, we show the case of $n_T = n_R = 2$, $L = 3$, $M = 2$

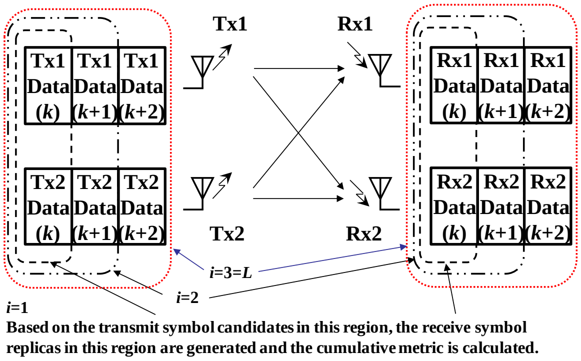

Fig. 7 Example of transmit and receive blocks ($n_T = 2$, $L = 3$, $M = 2$) in M algorithm

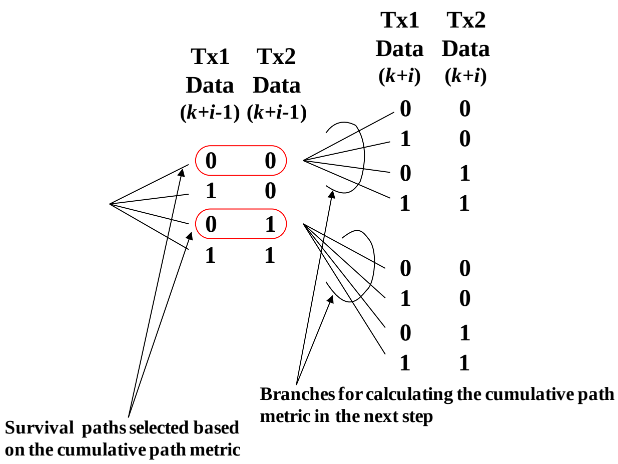

Fig. 8 Example of path selection in M algorithm ($n_T = 2$, $L = 3$, $M = 2$, $M_c = 2$)

and $M_c = 2$ in Fig. 7 and Fig. 8, as an example for simplicity.

<**Step1**> Calculation of cumulative path metric at $i = 1$ (Fig. 7)

<**Step2**> Based on the cumulative path metric at $i = 1$, $M_c (= 2)$ survival paths in the tree are selected. (Fig. 8)

<**Step3**> By increasing i one by one and repeating the step 1 and 2, the transmit data symbols with the survival path having the minimum cumulative path metric are determined at $i = L$.

Using the above mentioned M algorithm, the BER characteristics of proposed detection scheme, i.e., M algorithm with ISI canceller, is simulated with the simulation condition listed in Table III and is shown in Fig. 9. The delay profile between each transmit and receive antenna is the same as in Fig. 5.

From Fig. 9, the BER characteristics near MLD are obtained with the value $M_c = 16$ with less amount of calculation. Accordingly, we can say that the BER

Table III SIMULATION CONDITION IN FIG. 9

Modulation	M-ary FSK (M=4)
Modulation index: h	$h = 0.7$
Channel model between Tx and Rx antenna	Quasi-static Rayleigh fading channel with equal power 16 paths
Interval of delay $\Delta\tau$	$\Delta\tau = T_s / 8$
Number of antennas	MIMO 2×2
Channel estimation	Perfect at receiver
Signal separation and equalization	M-algorithm/MLD with ISI Canceller
Number of divisions in one symbol: $2c$ ($T_s = 2c\Delta t$)	$2c = 16$
Transmit block length $N_S T_s$	$4T_s$ ($N_S = 4$)
Length of ZP	$(L-1)T_s = 2T_s$

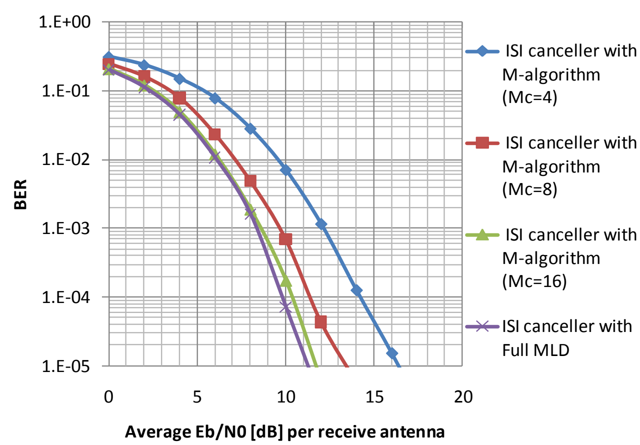

Fig. 9 BER characteristics of 4FSK (h=0.7) on MIMO 2×2 multipath channel

characteristics approaching the MLD are achievable by selecting the appropriate value of M_c .The amount of calculation of MLD is proportional to $M^{n_T L}$, while the one of M algorithm is M^{n_T} . Thus, we can cope with the channel with large symbol delay time of $(L-1)T_s$ and also can handle the larger modulation level of M .

IV. EVALUATION ON AMOUNT OF CALCULATION IN MIMO FSK RECEIVERS

The amount of calculation in MIMO MFSK receiver is estimated through the number of complex additions and multiplications for demodulating one transmit symbol. In Table IV, the numbers of complex additions and multiplications per one symbol for MIMO FSK detection schemes are shown, where we set $n_T = n_R$ and the approximation of $N_S \gg L$ is assumed with the notification of

$$A = 2c\left(2 \cdot J \cdot n_T + 3\right), \quad B = 2c\left(2 \cdot J \cdot n_R\right)L \qquad (16)$$

Under the condition in Table IV, the comparison of amount of calculation is evaluated and is shown in Fig. 10. When comparing the MLD with ISI canceller to the M algorithm with ISI canceller in Fig. 10, the amount of calculation of M algorithm with ISI canceller is far less than the MLD with

 ISBN: 978-1-61208-140-3

ISI canceller. Although the FDE with CP is superior to other two schemes in complexity, the BER characteristic is inferior to the other two. Considering the moderate amount of calculation at the receiver and the excellent BER characteristics, the proposed M algorithm with ISI canceller will be considered as the best choice.

TABLE IV NUMBER OF COMPLEX ADDITIONS AND MULTIPLICATIONS PER ONE SYMBOL TO BE DETECTED

FDE with CP	$2c\left[\begin{array}{l}10\log_2(2c\cdot N_S)\\ +2n_T^2+2n_T-13\end{array}\right]$
MLD with ISI canceller	$ALM^{n_T\times L}+B$
ISI canceller with M-algorithm	$A\cdot M^{n_T}\left\{1+M_c\cdot\frac{1}{2}(L^2+L-2)\right\}+B$

TABLE V CONDITIONS FOR EVALUATING THE AMOUNT OF CALCLATION IN FIG.10

Modulation	M-ary FSK (M= 4)
Modulation index: h	$h=0.7$
Channel model between Tx and Rx antenna	Quasi-static Rayleigh fading channel with equal power 16 paths
Interval of delay $\Delta\tau$	$\Delta\tau=T_s/8$
Number of antennas	MIMO 2×2
Channel estimation	Perfect at receiver
Number of divisions in one symbol: $2c$ ($T_s=2c\Delta t$)	$2c=16$
Length of ZP or CP	$2T_s$
Transmit block length $N_S T_s$	$N_S=8$

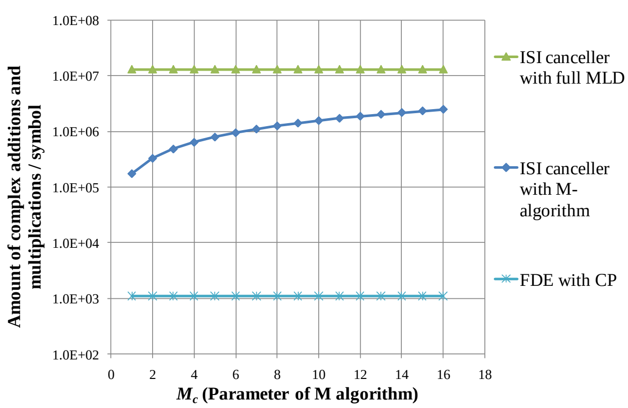

Fig. 10 Amount of calculation at the receiver (MIMO2×2, $\Delta\tau=T_s/8$)

V. CONCLUSIONS

We have proposed the MFSK receiver structure using M algorithm with ISI canceller on MIMO frequency selective channels. Our previously proposed receiver structure utilized the FDE with CP for signal separation and equalization before the demodulation of MFSK signal followed by energy detectors, however the BER characteristic of FDE scheme with CP was a little bit poor. To improve the BER characteristics of FDE with CP, we have investigated the receiver structure using MLD with ISI canceller which has the excellent BER characteristics. Although the MLD with ISI canceller exhibits the excellent BER characteristics, the amount of calculation at the receiver, which increases exponentially with the number of transmit antenna n_T and the MLD window size L, becomes large and is difficult actually to be implemented. In order to solve the complexity problem, the MLD is replaced by M algorithm. By selecting the appropriate value of M algorithm parameter M_c, the BER characteristic approaches the lowest value achievable by MLD. In the proposed M algorithm with ISI canceller, the receiver complexity increases exponentially only with the number of transmit antenna, thus we can reduce the receiver complexity. Accordingly the proposed receiver can cope with large delay time of multipath channels. We have developed the MIMO FSK receiver with low BER and modest complexity, which will be effective to increase the transmission rate of conventional SISO FSK channels. As a future study, the measurement of channel state information at the receiver will be needed to assess the actual BER degradation for practical applications.

ACKNOWLEDGEMENT

This study is partially supported by the Grants-in-Aid for Scientific Research 21560396 of the Japan Society for the Promotion of Science, the Telecommunications Advancement Foundation and the Sharp Corporation. The authors also acknowledge the helps of Dr. Eiji Okamoto and Mrs. Kazumi Ueda.

REFERENCES

[1] David Falconer, Sirikiat Lek Ariyavisitakul, Anader Benyamin-Seeyar, and Brian Eidson, "Frequency Domain Equalization for Single-Carrier Broadband Wireless Systems," *IEEE Commun. Mag*., pp.58-66, April 2002.

[2] Manabu Hijimoto, Yasunori Iwanami, and Eiji Okamoto, "A study on M-ary FSK with non-coherent detection on MIMO frequency selective channels," *Technical report of IEICE*, RCS2008-230, pp.107-112, Mar. 2009 (in Japanese).

[3] Kenji Nakayama , Yasunori Iwanami, and Eiji Okamoto, "A comparative study of MIMO-MFSK with frequency and energy detection under frequency-selective fading channels" , IEICE Society Conference, B-5-34, Sep. 2009 (in Japanese).

[4] Kenji Nakayama, Yasunori Iwanami, and Eiji Okamoto, "MIMO MFSK receivers using FDE and MLD on quasi-static frequency selective fading channels," International Symposium on Information Theory and its Applications 2010 (*ISITA2010*), Taichung Taiwan, ES2-Mo-1, 6 pages, Oct. 2010.

[5] Masahiro Maki and Yoshihiko Akaiwa, "An adaptive equalizer for FSK frequency detection," *IEICE Technical Report*, RCS 93-54, pp.23-28, September, 1993 (in Japanese).

[6] Satoshi Nakanobu, Yasunori Iwanami, and Eiji Okamoto, "A Comparative Study on Time Domain Sequential Equalizer with MLD and MLSE Equalizer on MIMO Frequency Selective Channels," *IEICE Trans. on Commun.*, vol.E93-B, No.11, pp.3197-3202, Nov. 2010.

[7] Yasunori Iwanami and Paul H. Wittke, "BER analysis of binary CP-FSK with energy detection and sequence estimation on frequency selective multipath channels", *International Conference on Communications* (*ICC'99*), Vancouver, S21.3, vol.2, pp.833-837, June 1999.

[8] Yasunori Iwanami and Paul H. Wittke, "Error Performance Analysis of an Energy Sequence Estimation Receiver for Binary FSK on Frequency-Selective Fading Channels, *IEEE Trans. on Wireless Communications*, Vol. 2, No. 2, pp. 260-269, March 2003.